Right Ventrolateral Prefrontal Cortex Mediates Individual Differences in Conflict-driven Cognitive Control

Tobias Egner

Abstract

■ Conflict adaptation—a conflict-triggered improvement in the resolution of conflicting stimulus or response representations—has become a widely used probe of cognitive control processes in both healthy and clinical populations. Previous fMRI studies have localized activation foci associated with conflict resolution to dorsolateral PFC (dlPFC). The traditional group analysis approach employed in these studies highlights regions that are, on average, activated during conflict resolution, but does not necessarily reveal areas mediating individual differences in conflict resolution, because between-subject variance is treated as noise. Here, we employed a complementary approach to elucidate the neural bases of variability in the proficiency of conflict-driven cognitive control. We analyzed two independent fMRI data sets of face–word Stroop tasks by using individual variability in the behavioral expression of conflict adaptation as the metric against which brain activation was regressed while controlling for individual differences in mean RT and Stroop interference. Across the two experiments, a replicable neural substrate of individual variation in conflict adaptation was found in ventrolateral PFC (vlPFC), specifically, in the right inferior frontal gyrus, *pars orbitalis* (BA 47). Unbiased regression estimates showed that variability in activity in this region accounted for ~40% of the variance in behavioral expression of conflict adaptation across subjects, thus documenting a heretofore unsuspected key role for vlPFC in mediating conflict-driven adjustments in cognitive control. We speculate that vlPFC plays a primary role in conflict control that is supplemented by dlPFC recruitment under conditions of suboptimal performance. ■

INTRODUCTION

The detection and resolution of interference (or conflict) in goal-directed processing by task-irrelevant stimulus or response representations is considered a major function of cognitive (or executive) control (Fuster, 2008; Botvinick, Braver, Barch, Carter, & Cohen, 2001; Shallice & Burgess, 1996; Norman & Shallice, 1986), and considerable evidence suggests that this function falls under the purview of the frontal lobes (Fuster, 2008; Botvinick et al., 2001; Miller & Cohen, 2001; Stuss, Floden, Alexander, Levine, & Katz, 2001; Shallice & Burgess, 1996; Stuss & Benson, 1984). One elegant probe of the integrity and neural bases of such conflict resolution processes is provided by the "conflict adaptation effect" observed in classic tests of executive function, such as the Stroop task (for a review, see Egner, 2007). As an example, consider the face–word Stroop task employed in one experiment of the current study (Egner, Etkin, Gale, & Hirsch, 2008): On each trial, the subject is required to categorize a pictorial stimulus consisting of a male or female face according to its gender. Each face stimulus is overlaid with a written gender label ("male" or "female") that can either be semantically congruent or incongruent with the face's gender. Subjects typically exhibit slower responses and higher error rates to incongruent than to congruent stimuli (the classic interference or conflict effect), and this decline in performance is thought to reflect the cost of the recruitment of cognitive control resources necessary for resolving the interference from conflicting stimulus information.

Conflict adaptation refers to the frequent finding of a reduction in this interference effect following an incongruent trial compared with a congruent one (Gratton, Coles, & Donchin, 1992). The prevalent interpretation of this effect is that conflict in information processing in trial $n - 1$ triggers an up-regulation in cognitive control (corresponding to reinforcing the working memory representation of the current task set), which increases top–down biasing of task-relevant over task-irrelevant stimulus representations, thus improving conflict resolution on trial n (Botvinick et al., 2001). Conflict adaptation has begun to be employed as a tool for gauging specific cognitive and neural dysfunction in psychiatric (e.g., Kerns et al., 2005) and neurological (e.g., di Pellegrino, Ciaramelli, & Ladavas, 2007; Fellows & Farah, 2005) patient populations, and to basic cognitive neuroscience researchers, it has offered the opportunity of segregating brain regions whose activity is more closely tied to the occurrence and detection of conflict (more active on incongruent trials following a congruent trial or "CI trials") from those that are implicated in adapting to that conflict, that is, in conflict resolution proper (more active on incongruent trials

Duke University, Durham

following an incongruent trial or "II trials"). Pursuing this approach, a number of neuroimaging studies have investigated the neural substrates of the conflict resolution process in Stroop-type tasks and have implicated (typically right hemisphere) dorsolateral regions of the PFC (dlPFC) as mediating conflict-driven up-regulation in top–down control (Egner et al., 2008; Egner & Hirsch, 2005a, 2005b; Kerns et al., 2004).

One commonality among previous imaging studies of conflict resolution is that activation foci were identified as a function of mean group activation contrasts, detecting regions that are, on average across the group of subjects, more activated in a condition of high cognitive control than in a comparison condition of low cognitive control (i.e., via a group contrast of II > CI trials). These contrasts treat variability across individuals as noise, because between-subject variance contributes to the error term of the statistical analysis. By disregarding information concerning individual differences in the expression of the behavioral conflict adaptation effect (which tend to be substantial), the standard group statistic might, therefore, overlook key brain regions contributing to conflict resolution. Specifically, the mean group statistic does not necessarily detect areas that are directly linked to the proficiency of conflict-driven control across subjects (although the regions identified via the mean group statistic could, in principle, be such areas). The latter can be achieved by utilizing individual differences in behavior as a predictor of brain activation across subjects. Here, regions mediating the relative proficiency of conflict-driven control would display higher conflict-triggered activation in subjects who exhibit higher levels of behavioral conflict adaptation, and lower activation in subjects displaying lower levels of conflict adaptation. Identifying neural substrates of cognitive control processes by means of individual difference analyses has begun to produce important new insights into the functional organization of cognitive control processes (e.g., Forstmann, Jahfari, et al., 2008; Forstmann, van den Wildenberg, & Ridderinkhof, 2008) and is particularly desirable from a clinical perspective, where differences rather than commonalities in function across subjects represent the major currency for understanding abnormal neural and psychological processes.

To test for brain regions that may reliably mediate the proficiency of conflict-driven interference resolution across subjects, in the present study we performed a reanalysis of two independent, previously published data sets of face–word Stroop tasks (Egner et al., 2008; Egner & Hirsch, 2005a), which in the following will be referred to as Experiment 1 (Egner & Hirsch, 2005a) and Experiment 2 (Egner et al., 2008). The previous analyses on these data sets employed II > CI trial contrasts in traditional mean group statistics and documented that, on average, conflict-driven enhancement in cognitive control was associated with enhanced activity in right dlPFC (Egner et al., 2008; Egner & Hirsch, 2005a; for similar results, see Kerns et al., 2004). In the current study, we asked the question whether the intersubject variability in behavioral conflict adaptation that was ignored in the previous analyses could be explained to a significant degree by variability in conflict-driven activation in a particular brain region. The fact that we had two independent data sets stemming from similar (but not identical) Stroop protocols at our disposal furthermore allowed us to gauge whether any potential brain–behavior associations were truly robust, that is, whether they were replicable across studies. To this end, we analyzed separately the data from Experiments 1 and 2, using individual variability in the behavioral expression of conflict adaptation as the metric against which conflict-driven brain activation (II > CI trial activity) was regressed. To isolate neural correlates specific to the conflict resolution process itself, the regression models also included nuisance regressors that accounted for individual differences in mean RT and mean Stroop interference scores. To preview the results, we observed a reliable association between individual differences in behavioral conflict adaptation and conflict-driven activation in the right ventrolateral PFC (vlPFC), specifically, the orbital aspect of the right inferior frontal gyrus (IFG).

METHODS

Experiment 1

Subjects

Twenty-two (14 women) healthy volunteers (mean age = 28.7 years, range = 20–40 years) gave written informed consent in accordance with institutional guidelines to participate in this study.

Experimental Protocol

Stimuli were presented with Presentation software (Neurobehavioral Systems, nbs.neuro-bs.com), and displayed with a back-projection screen that was viewed by the subjects via a mirror attached to the head coil. The main task consisted of 148 presentations of photographic stimuli on a black background, depicting the face of either an actor (Robert DeNiro, Al Pacino, or Jack Nicholson) or a political figure (Fidel Castro, Bill Clinton, or Mao Zedong), all of whom were readily identified by the subjects before the experiment. Faces were presented with category-congruent (e.g., the face of an actor paired with the name of an actor) or category-incongruent (e.g., the face of an actor paired with the name of a politician) names written across them in red letters. An example of a category-incongruent stimulus is shown in Figure 1A. No face–stimulus was paired with its own name. Stimuli were presented for 1000 msec, with a varying ISI of 3000–5000 msec (mean ISI = 4000 msec), in pseudorandom order (counterbalanced for equal numbers of congruent–congruent [CC], congruent–incongruent [CI], incongruent–congruent [IC], and incongruent–incongruent [II] stimulus sequences). Stimulus occurrences were counterbalanced across trial types and response buttons. Alternative

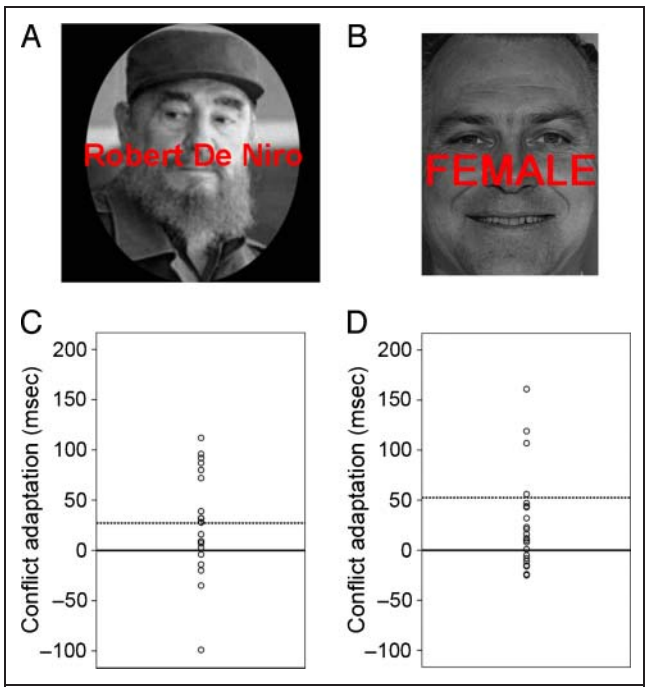

Figure 1. Example stimuli and individual variation in the expression of the conflict adaptation effect (the differential in the congruency effect following an incongruent as compared with a congruent trial) are shown for Experiment 1 (A, C) and Experiment 2 (B, D). In C and D, each individual subject's conflict adaptation score (in msec) is shown as a circle, with solid lines marking zero conflict adaptation, and dashed lines marking the mean conflict adaptation score for each sample. Positive values reflect reduced interference following an incongruent compared with a congruent trial, that is, successful conflict adaptation.

sources of trial sequence effects, other than conflict, notably repetition priming (Mayr, Awh, & Laurey, 2003), and "partial repetition" effects (Hommel, Proctor, & Vu, 2004), were controlled for in the current study, as target stimuli always alternated across trials, and the proportion of response and distracter repetitions to response and distracter alternations was the same (50%) for all trial sequence types. There were no cases where a previous trial distracter feature became a current trial target feature, thus avoiding negative priming effects. Furthermore, we have previously shown that this task does not incur "category-priming" effects stemming from repetitions of a given face or word category (Egner & Hirsch, 2005a). It was the subjects' task to categorize the pictorial face stimuli according to category (actor vs. politician). Subjects were instructed to respond as fast as possible, while maintaining accuracy, by pushing response buttons corresponding to "actor" (right index finger) or "politician" (right middle finger).

Behavioral Data Analysis

Behavioral data analysis focused on mean RTs, which excluded error and posterror trials and condition-specific outlier values of more than 2 standard deviations from the mean. For the purpose of the individual difference fMRI analysis, conflict adaptation scores were calculated for each subject. In the behavioral literature, it is customary to express this effect via the full Previous × Current trial congruency interaction term ([CI–CC]–[II–IC]), whereas in neuroimaging studies researchers have tended to focus exclusively on incongruent trials, that is, the difference between CI and II trials. To accommodate both of these emphases, we calculated both types of behavioral adaptation score for each subject. In other words, we computed both the full interaction term ([CI–CC]–[II–IC]), reflecting the degree to which an individual's current trial interference effect varied as a function of previous trial congruency (with positive values reflecting a decrease in interference), as well as a (CI–II) score, reflecting the decrease in RT to incongruent trials following an incongruent compared with a congruent stimulus, which is equivalent to the contrast used in the imaging analysis. Each subject's mean RT as well as their mean Stroop interference scores (all incongruent trials minus all congruent trials) were also calculated for the purpose of the fMRI analysis (see *Image Analysis* below).

Image Acquisition

Images were recorded with a GE 1.5-T scanner. Functional images were acquired parallel to the AC–PC line with a T2*-weighted EPI sequence of 24 contiguous axial slices (repetition time [TR] = 2000 msec, echo time [TE] = 40 msec, flip angle = 60°, field of view [FoV] = 190 × 190 mm, array size = 64 × 64) of 4.5-mm thickness and 3 × 3 mm in-plane resolution. Structural images were acquired with a T1-weighted SPGR (spoiled gradient recalled acquisition) sequence (TR = 19 msec, TE = 5 msec, flip angle = 20°, FoV = 220 × 220 mm), recording 124 slices at a slice thickness of 1.5 mm and in-plane resolution of 0.86 × 0.86 mm.

Image Analysis

All preprocessing and statistical analyses were carried out using SPM2 (www.fil.ion.ucl.ac.uk/spm/spm2.html). Functional data were corrected for differences in slice timing, spatially realigned to the first volume of the first run. The realigned images were spatially normalized to the Montreal Neurological Institute (MNI) template brain (resampled voxel size = 2 mm^3) before smoothing with an 8 mm^3 FWHM (full-width half-maximum) kernel. The first five volumes of each run were discarded before building and estimating the statistical model of the task. A 128-sec temporal high-pass filter was applied to the data and models. Temporal autocorrelations were estimated using restricted maximum likelihood estimates of variance components using a first-order autoregressive model (AR-1), and the resulting nonsphericity was used to form maximum likelihood estimates of the activations.

For the main task analysis, regressors were formed through vectors of stick functions (convolved with a

canonical HRF [hemodynamic response function]) corresponding to the stimulus onsets for each condition (CC, CI, IC, II), with error and posterror trials modeled separately. Neural correlates of conflict-driven cognitive control were identified at the single-subject level by contrasting event-related activity between II and CI trials (II > CI). The II > CI contrast image for each subject was subsequently entered into a second-level random effect group regression analysis, together with each subject's behavioral conflict adaptation scores (see *Behavioral Data Analysis* above), as well as each individual's mean RT and mean Stroop interference score. The latter two variables acted as nuisance regressors that controlled for individual differences in general response speed and susceptibility to conflict per se. The group regression analysis result of interest stemmed from a contrast weighting the conflict adaptation score with "1" and all other regressors with "0." This analysis reveals voxels whose conflict-driven activity covaried positively with individuals' degree of behavioral conflict adaptation. This analysis was performed once using the full conflict adaptation interaction term ([CI–CC]–[II–IC]) as the behavioral metric of conflict adaptation and once using the conflict-modulated performance in incongruent trials only (CI–II) as the behavioral metric of conflict adaptation. The regression analysis was performed over a whole-brain search space that was constrained by a gray matter mask (dilated by a factor of 1.5 to accommodate voxels at the interface between gray matter and white matter), using the WFU PickAtlas software (fmri.wfubmc.edu/software/PickAtlas). For the resulting search space, combined voxel height and cluster extent thresholds corrected for multiple comparisons were determined by using the 3dClustSim code of the AlphaSim program of the AFNI analysis suite (afni.nimh.nih.gov/pub/dist/doc/program_help/3dClustSim.html). Specifically, the program was used to run a set of simulations that take into account the size of the search space and the estimated smoothness of the data to generate probability estimates (based on simulated data) of a random field of noise producing a cluster of voxels of a given size for a set of voxels passing a given voxelwise p value threshold. The simulations determined that, for the Experiment 1 data, a combined voxelwise p value of <0.005 and a cluster size of >21 voxels would correspond to a multiple-comparison corrected combined threshold of $p < .05$.

Experiment 2

Subjects

Twenty-two (14 women) right-handed healthy volunteers (mean age = 26.6 years, SD = 5.4 years) gave written informed consent to participate in this study in accordance with institutional guidelines. All participants had normal or corrected-to-normal vision and were screened by self-report to exclude any subjects reporting previous or current neurological or psychiatric conditions and current psychotropic medication use.

Experimental Protocol

Stimuli were presented with Presentation software (Neurobehavioral Systems, nbs.neuro-bs.com) and displayed on a back-projection screen that was viewed by the subjects via a mirror attached to the head coil. Each trial consisted of a photographic stimulus on a black background, depicting either a male or female face (Ekman & Friesen, 1976). (Each face also displayed either a happy of fearful emotional expression, but this stimulus feature was irrelevant to the task described here). The stimulus set consisted of five male faces and five female faces. Face stimuli were presented with either the word "MALE" or "FEMALE" superimposed in red letters, producing gender-congruent and gender-incongruent stimuli. An example of a gender-incongruent stimulus is displayed in Figure 1B. Subjects were required to categorize the faces as being of either male or female gender while trying to ignore the task-irrelevant word stimuli. Responses consisted of manual button presses (right index finger for men, right middle finger for women), and subjects were instructed to respond as fast as possible while maintaining high accuracy. The task consisted of one run of 148 trials. Stimuli were presented for 1000 msec, with a varying ISI of 3000–5000 msec (mean ISI = 4000 msec), during which a white central fixation cross was displayed on a black background. Stimuli were presented in pseudorandom order (counterbalanced for equal numbers of CC, CI, IC, and II trial sequences). Gender and facial expression were counterbalanced across responses and trial types in both tasks. Alternative sources of trial sequence effects, other than conflict, notably repetition priming (Mayr et al., 2003) and "partial repetition" effects (Hommel et al., 2004), were controlled for in the current study, as target stimuli always alternated across trials, and the proportion of response and distracter repetitions to response and distracter alternations was the same (50%) for all trial sequence types. There were no cases where a previous trial distracter feature became a current trial target feature, thus avoiding negative priming effects. Furthermore, we have previously shown that this type of task does not incur "category-priming" effects stemming from repetitions of a given face category and word category (Etkin, Egner, Peraza, Kandel, & Hirsch, 2006; Egner & Hirsch, 2005a).

Behavioral Data Analysis

Behavioral data analyzed consisted of RT (excluding error and posterror trials and trimmed to exclude outlier values of more than 2 standard deviations from the mean). As in Experiment 1 (see above), we calculated individual mean RT, mean Stroop interference scores, and conflict adaptation scores.

Image Acquisition

Images were recorded with a GE 1.5-T scanner. Functional images were acquired parallel to the AC–PC line with a

T2*-weighted EPI sequence of 24 contiguous axial slices (TR = 2000 msec, TE = 40 msec, flip angle = 60°, FoV = 190 × 190 mm, array size = 64 × 64) of 4.5 mm thickness and 3 × 3 mm in-plane resolution. Structural images were acquired with a T1-weighted SPGR sequence (TR = 19 msec, TE = 5 msec, flip angle = 20°, FoV = 220 × 220 mm), recording 124 slices at a slice thickness of 1.5 mm and in-plane resolution of 0.86 × 0.86 mm.

Image Analysis

All preprocessing and statistical analyses were carried out using SPM2 (www.fil.ion.ucl.ac.uk/spm/spm2.html). Functional data were slice time corrected and spatially realigned to the first volume of the first run. The structural scan was coregistered to the functional images and served to calculate transformation parameters for spatially warping functional images to the MNI template brain (resampled voxel size = 2 mm^3). Finally, normalized functional images were spatially smoothed with an 8 mm^3 kernel. The first five volumes of each run were discarded before building and estimating the statistical models. To remove low-frequency confounds, data were high-pass filtered (128 sec). Temporal autocorrelations were estimated using restricted maximum likelihood estimates of variance components using a first-order autoregressive model (AR-1), and the resulting nonsphericity was used to form maximum likelihood estimates of the activations.

As in Experiment 1, for the main task analysis, stick function regressors for stimulus events (convolved with a canonical HRF) were created for stimulus onsets of CC, CI, IC, and II trial types, with error and posterror trials modeled separately. Neural correlates of conflict-driven cognitive control were identified at the single-subject level by contrasting event-related activity between II and CI trials (II > CI). The II > CI contrast image for each subject was subsequently entered into a second-level random effect group regression analysis, together with each subject's behavioral conflict adaptation scores, as well as each individual's mean RT and mean Stroop interference score. The group regression analysis result of interest stemmed from a contrast weighting the conflict adaptation score with "1" and all other regressors with "0." This analysis reveals voxels whose conflict-driven activity covaried positively with individuals' degree of behavioral conflict adaptation. This analysis was performed once using the full conflict adaptation interaction term ([CI–CC]–[II–IC]) as the behavioral metric of conflict adaptation and once using the conflict-modulated performance in incongruent trials only (CI–II) as the behavioral metric of conflict adaptation. As in Experiment 1, the regression analysis was performed over a whole-brain search space that was constrained by a gray matter mask and multiple-comparison correction was performed using AlphaSim simulations (see above). The simulations determined that, for the Experiment 2 data, a combined voxelwise p value of <0.005 and a cluster size of >35 voxels would correspond to a multiple-comparison corrected combined threshold of $p < .05$.

RESULTS

Behavioral Data

As reported previously (Egner et al., 2008; Egner & Hirsch, 2005a), both experiments were associated with significant mean conflict adaptation effects across subjects (Previous × Current trial congruency interaction, Experiment 1: $F(1, 21) = 6.7$, $p < .05$; Experiment 2: $F(1, 21) = 6.9$, $p < .05$), as the magnitude of congruency effects was decreased following incongruent trials compared with following congruent ones. Descriptive RT data for all conditions in both experiments are reported in Table 1. Most pertinent for the present purpose, in both samples, there was a substantial amount of individual variability in the expression of this effect, ranging from highly reduced to moderately increased interference scores following incongruent trials, as shown in Figure 1C (Experiment 1) and D (Experiment 2). The key question then was whether this variability in behavioral conflict adaptation could be explained in part by variability in conflict-driven activation in a particular brain region and whether the same brain region would mediate this variability across two independent samples performing similar, but not identical, face–word Stroop tasks.

Brain–Behavior Correlation Data

As detailed in previous publications (Egner et al., 2008; Egner & Hirsch, 2005a), mean group effects for the II > CI contrast, aimed at revealing neural substrates of conflict-driven control, exposed activation foci in right dorsolateral prefrontal regions, corresponding to right middle frontal gyrus in BA 46 (Egner & Hirsch, 2005a) and right superior frontal gyrus in BA 9 (Egner et al., 2008; data not shown). For the present purpose, the II > CI contrast images of each subject were entered into group regression analyses with the subjects' behavioral conflict adaptation scores ([CI–CC]–[II–IC]). To control for brain–behavior associations driven by overall differences in response speed or mean Stroop interference across subjects, the latter RT variables were also entered into the regression analyses

Table 1. Descriptive Statistics of Behavioral Data

	Experiment 1		*Experiment 2*	
	RT (msec)	*SD*	*RT (msec)*	*SD*
CC	705	74	679	118
CI	732	81	746	191
IC	717	76	682	118
II	717	77	721	158

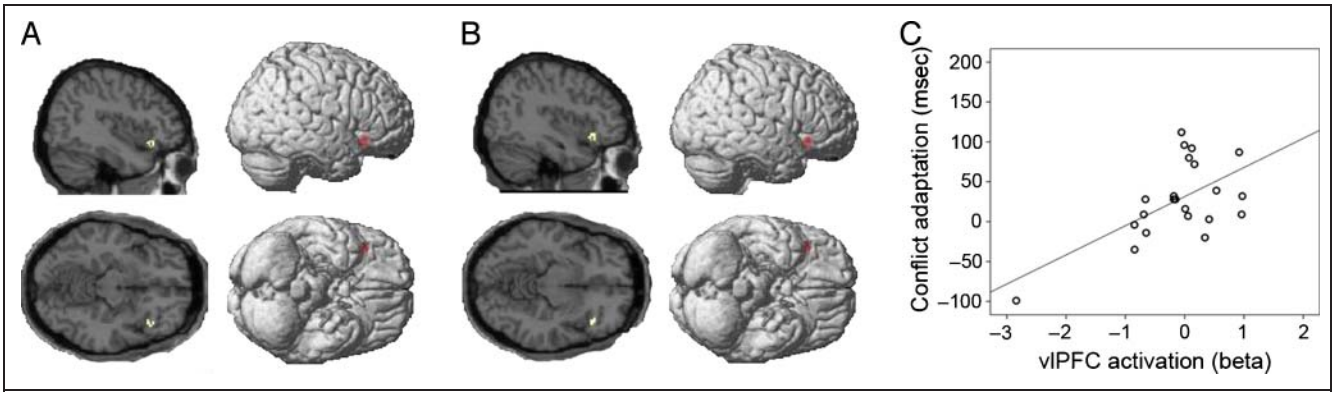

Figure 2. (A, B) Experiment 1 neuroimaging results for a whole-brain search for voxels displaying a positive correlation between conflict-driven neural activity and behavioral conflict adaptation scores, as defined by the Previous × Current trial congruency interaction term ([CI–CC]–[II–IC]; A) or as defined by the relative speed-up on incongruent trials only (CI–II; B) is shown on sagital and axial slices (left) and rendered (right) on a normalized brain (voxelwise height threshold = $p < .005$, cluster extent threshold > 21 voxels). (C) Unbiased regression estimate (see Methods) of the association between intersubject variability in behavioral conflict adaptation ([CI–CC]–[II–IC]; *y* axis) and conflict-driven activity in the right vlPFC (*x* axis).

and treated as nuisance variables. The analysis of the Experiment 1 data yielded a single suprathreshold cluster of activation (at $p < .05$, corrected) located in right vlPFC (Figure 2A), corresponding to the *pars orbitalis* of the inferior frontal gyrus (IFG) in BA 47 (or area 47/12, according to Petrides & Pandya, 1994). Activation in this region displayed a positive correlation with behavioral conflict adaptation, in that subjects with higher conflict-driven right IFG activity tended to exhibit higher behavioral adjustments following incongruent trials. We also carried out the same analysis but using as behavioral regressor the performance on incongruent trials only, that is, the subjects' relative speed-up on II as compared with CI trials (CI–II). This regression analysis produced essentially equivalent results, isolating a closely overlapping activation cluster in right IFG (see Figure 2B).

To test whether this association between right vlPFC activity and conflict adaptation scores represents a replicable phenomenon, we conducted the same analysis on the independent imaging data of Experiment 2. Again, a cluster of suprathreshold activation ($p < .05$, corrected) was observed in the orbital aspect of the right IFG (Figure 3A), in proximity of the cluster detected in the previous sample (cf. Figure 2A). In contrast to the prior data set, however, additional suprathreshold associations were also found in the left posterior parietal cortex (inferior parietal lobule, BA 40). Like in Experiment 1, we carried out an additional analysis that employed the (CI–II) RT differential as the behavioral regressor. Again, this analysis produced basically equivalent results in the right vlPFC, isolating a closely overlapping activation cluster in the right IFG (see Figure 3B). In addition to that region, this analysis also highlighted a more dorsal and posterior cluster of activation that bridged the right precentral gyrus (BA 6) and the very posterior and superior aspect of the IFG (BA 9), as well as a cluster in the right superior parietal lobule (BA 7).

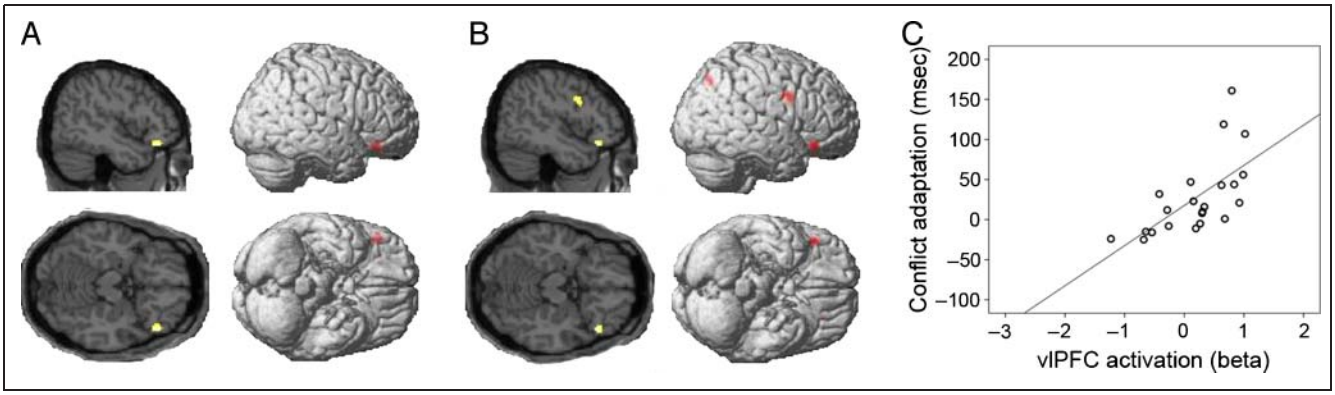

Figure 3. (A, B) Experiment 2 neuroimaging results for a whole-brain search for voxels displaying a positive correlation between conflict-driven neural activity and behavioral conflict adaptation scores, as defined by the Previous × Current trial congruency interaction term ([CI–CC]–[II–IC]; A) or as defined by the relative speed-up on incongruent trials only (CI–II; B), are shown on sagital and axial slices (left) and rendered (right) on a normalized brain (voxelwise height threshold = $p < .005$, cluster extent threshold > 35 voxels). (C) Unbiased regression estimate (see Methods) of the association between intersubject variability in behavioral conflict adaptation ([CI–CC]–[II–IC]; *y* axis) and conflict-driven activity in the right vlPFC (*x* axis).

All significant activation foci across the two experiments are reported in Table 2.

To summarize the above results, it was found that individual differences in the behavioral expression of conflict-driven cognitive control were reliably associated with intersubject variability in the level of activation of the right vlPFC across two independent subject cohorts performing two different variants of a face–word Stroop task and regardless of the precise behavioral metric of conflict adaptation used. In fact, intersubject variability in conflict-driven activity across the (largely overlapping) clusters identified either by the Previous × Current trial congruency interaction ([CI–CC]–[II–IC]) regressor or the relative speed-up on incongruent trials only (CI–II) regressor was extremely highly correlated in both experiments (Experiment 1: $r = .99$, $p < .001$; Experiment 2: $r = .96$, $p < .001$). In view of this finding, we limited all subsequent analyses to the clusters identified with the full conflict adaptation interaction ([CI–CC]–[II–IC]) scores only.

To estimate (and display) the strength of the associations between behavioral conflict adaptation effects and conflict-induced changes in right vlPFC in a manner that is free from selection bias or circular "double-dipping" effects (Kriegeskorte, Simmons, Bellgowan, & Baker, 2009), we extracted data and computed correlations using an iterative "leave-one-subject-out" approach. Specifically, for each subject, an ROI in the right IFC was defined on the basis of the brain–behavior correlation results from all other subjects, but excluding that subject's own data. In this way, the ROI data that were extracted from each subject for the purpose of the correlation analyses did not actually contribute to the selection criteria that defined that subject's ROI data in the first place, thus rendering data selection and analysis independent of each other.

Table 2. Brain Regions Whose Conflict-driven Activation Was Associated with Behavioral Conflict Adaptation across Individuals

	BA	*MNI (x, y, z)*	*Cluster*	*Z score*
Experiment 1 ([CI–CC]–[II–IC])				
IFG	47	42, 24, −12	32	3.13
Experiment 1 (CI–II)				
IFG	47	40, 26, −10	30	3.30
Experiment 2 ([CI–CC]–[II–IC])				
IFG	47	48, 32, −16	44	3.67
Inferior parietal lobule	40	−50, −42, 48	165	3.59
Experiment 2 (CI–II)				
IFG	47	48, 28, −16	38	3.51
Precentral gyrus/IFG	6/9	40, 6, 28	102	3.52
Superior parietal lobule	7	34, −70, 46	39	3.00

BA = probable Brodmann's area; MNI = MNI coordinates of peak activation voxel in each cluster; cluster = number of suprathreshold voxels in cluster.

In Experiment 1, the Pearson correlation coefficient between behavioral conflict adaptation ([CI–CC]–[II–IC]) and right IFG cluster activity defined via individual differences in the equivalent adaptation score was .60 ($p < .005$), corresponding to an R^2 (variance accounted for) of .36 (Figure 2C). In Experiment 2, the corresponding correlation was .65 ($p = .001$), resulting in an R^2 of .42 (Figure 3C). In other words, individual variability in right IFG activity following high-conflict trials explained between 36% and 42% of the variance in behavioral conflict adaptation effects. To ascertain that the associations between conflict adaptation and IFG activity were not unduly driven by any one subject, these analyses were rerun with an iterative leave-one-subject-out approach (i.e., testing all possible combinations of 21 of 22 subjects for each sample). Each permutation of these correlation analyses remained statistically significant ($p < .05$) for both experiments. Thus, the present data document a reliable role for the right vlPFC in mediating individual differences in conflict-driven cognitive control.

Relationship to Mean Group Activation Effects

An interesting post hoc question with regard to the above findings concerns the relationship between individual variation in behavioral adaptation as well as conflict-driven activity in the right vlPFC region identified here and individual differences in the conflict-driven activation of the dlPFC foci identified in the traditional mean group analyses of the same data sets. As noted above, the mean group II > CI contrasts in both samples had revealed activity in right dlPFC regions (BA 46/9; Egner et al., 2008; Egner & Hirsch, 2005a). To explore how conflict-driven activation in these dlPFC regions might relate to behavioral conflict adaptation success and to variance in activity of the vlPFC locus identified in the current article, we performed additional regression analyses. Specifically, individual beta estimates for II > CI contrasts for vlPFC and dlPFC foci (the latter based on Egner et al., 2008; Egner & Hirsch, 2005a) were entered as predictors of behavioral conflict adaptation in stepwise regression analyses (inclusion criterion $p < .05$, exclusion criterion $p > .1$), for each data set.

For Experiment 1, it was found that the inclusion of the dlPFC locus in the regression model accounted for significant additional variance in the behavioral data. In particular, although the vlPFC activity on its own produced an R^2 of .36 ($p < .005$), the addition of the dlPFC activation in the model raised the R^2 to .54 ($p < .05$). Interestingly, in contrast to the positive vlPFC–behavior correlation, the contribution of the conflict-driven dlPFC responses to the model was based on a significant negative relationship between activity at this site and the behavioral adaptation effect ($r = -.37$, $p < .05$). For Experiment 2, dlPFC did not

significantly improve the regression model based on the vlPFC data alone ($R^2 = .42$, $p = .001$). However, descriptively similar to Experiment 1, variability in conflict-driven dlPFC activity again tended to be negatively correlated with behavioral adaptation effects ($r = -.27$), although this relationship was not statistically robust ($p > .1$).

DISCUSSION

The goal of the current study was to identify the neural substrates of individual variability in the behavioral expression of conflict-driven cognitive control, known as conflict adaptation. To this end, two independent fMRI data sets of conflict adaptation in face–word Stroop protocols were analyzed in regression analyses that employed individual variability in behavioral conflict adaptation as the predictor of variance in conflict-driven brain activity. Although previous analyses that pursued a traditional mean group activation approach to delineating neural substrates of conflict adaptation had implicated predominantly dorsolateral regions of the right PFC in this process (Egner et al., 2008; Egner & Hirsch, 2005a; Kerns et al., 2004), we here observed, across two independent samples, a replicable locus of association between conflict-driven brain activity and proficient behavioral adaptation in right vlPFC, specifically, the right IFG, pars orbitalis, corresponding to BA 47 (or Area 47/12 in the scheme of Petrides & Pandya, 1994). Subjects who displayed greater conflict-driven activity in this region tended to exhibit a greater degree of behavioral adaptation following conflicting stimuli, regardless of whether behavioral conflict adaptation was defined as the degree to which an individual's current trial interference effect varied as a function of previous trial congruency ([CI–CC]–[II–IC]) or as the relative decrease in RT to incongruent trials following an incongruent compared with a congruent stimulus (CI–II). Unbiased regression estimates indicated that variability in activity in right IFG accounted for about 40% of the variance in behavioral expression of conflict adaptation across subjects. These data firmly imply a previously unsuspected key role for the right vlPFC in facilitating proficient conflict-triggered interference control. Surprisingly, we also found that intersubject variability in activation of the dlPFC regions that display significant conflict-triggered activation in standard mean group analyses actually tends to correlate negatively with individuals' behavioral success at resolving conflict. In the following, we reflect speculatively on possible respective roles of the right ventrolateral and dlPFC in conflict adaptation.

First, regardless of specific anatomical considerations, one can infer potential functional roles for the frontal regions identified above by considering their relationship with behavioral adaptation success. The right dlPFC is reliably activated in mean group analyses of conflict adaptation (Egner et al., 2008; Egner & Hirsch, 2005a; Kerns et al., 2004) but nevertheless was here found to display a tendency of negative association with behavioral success at adaptation (see Results). This apparent contradiction can be explained by the assumption that this region is recruited in particular when subjects are struggling to resolve conflict, and its conflict-driven activation is, therefore, on average greater in those subjects who have greater difficulty in adapting to conflict than in those who adapt more proficiently, with the former subjects driving the mean group activation effects observed for this region. By contrast, conflict-triggered activity in the right vlPFC displays a close positive correlation with behavioral adaptation, which suggests a more primary role for this region than for dlPFC in controlling stimulus conflict. The fact that the vlPFC locus is not typically detected in mean group analyses implies that, for whatever reason, its recruitment is overall associated with less metabolic demand and/or displays a greater degree of variability across subjects. Our finding underlines the general importance of pursuing complementary individual difference analyses in fMRI studies. When considered side by side, the relationships of activation profiles in right dlPFC and vlPFC regions and behavior could be interpreted as suggesting that the right vlPFC is the primary source of on-line conflict control in the Stroop-type protocols employed in our experiments and that the right dlPFC is recruited additionally in case of performance difficulty and, thus, particularly in subjects who are struggling to adapt to conflict. We will next consider how these hypothetical functional roles relate to anatomical considerations and relevant models of functional parcelation of PFC.

In terms of its anatomical milieu, the vlPFC site highlighted in this study (BA 47) is distinguished most clearly from the adjacent more superior and posterior aspects of the IFG (BA 44/45), as well as from dlPFC (BA 9/46), by its dense connectivity with the rostral inferior temporal visual association cortex via the uncinate fasciculus (Petrides & Pandya, 2002b; Carmichael & Price, 1995; Barbas, 1988). This close connectivity with the apex of the ventral visual stream and its juxtaposition with the dlPFC (BA 46/9) regions' connectivity with parietal regions of the dorsal visual stream and the cingulate cortex have informed two of the more influential models of the functional neuroanatomy of PFC (Petrides, 1994; Goldman-Rakic, 1987), which in turn represent interesting candidate frameworks for the interpretation of the current results.

In Goldman–Rakic's classic "domain specificity" view of prefrontal organization, the dorsal and ventral regions at the focus of our discussion would be considered to support functionally equivalent working memory processes that temporarily represent information in the spatial versus nonspatial (object- or feature-based) domains, respectively (Goldman-Rakic & Leung, 2002; Goldman-Rakic, 1996; Goldman-Rakic, 1987). If we consider conflict adaptation a mechanism for task-set maintenance (Egner, 2008), that is, a conflict-induced reinforcement of a working memory representation of current task demands and associated top–down biases (Botvinick et al.,

2001), then the involvement of a region that is said to mediate object- or feature-based working memory processes (the vlPFC) in conflict adaptation would appear to be a sensible fit. This is particularly true given the nature of the experimental tasks at hand, namely, face–word Stroop protocols, where processing of both the relevant and irrelevant stimulus dimensions can be confidently attributed to regions of the ventral visual stream (Cohen et al., 2000; Kanwisher, McDermott, & Chun, 1997). However, the implied involvement of working memory processes in the spatial domain (dlPFC) in these protocols seems less straightforward to explain. The stimulus features (and the conflict they engender) have no obvious spatial characteristics and occupy largely overlapping locations, such that the Stroop-type protocols we employed would a priori be considered to be nonspatial tasks. However, it is at least theoretically possible that subjects could employ a narrow spatial focus on parts of the face stimuli that are not overlaid by the word stimuli to improve conflict resolution. From this somewhat labored perspective, the natural (and optimal) strategy for interference control in these tasks may be to employ object-based working memory representations in the vlPFC for the top–down biasing of the (non-spatial) stimulus features, but in case of exceptional performance difficulty, this strategy may be supplemented with attempts at spatial biasing that involve the dlPFC.

An alternative account for the functional roles of these regions is offered by the "process specificity" model of PFC, by Petrides and colleagues (Petrides, 1994, 1996, 2005; Petrides & Pandya, 2002a). This model views the (mid-) vlPFC (Area 47/12) as the primary interface of PFC with posterior sensory association cortices that is involved in "first-order" executive processes, including the selection, retrieval, and strategic regulation of (and judgments on) information in posterior regions. By contrast, the (mid-) dlPFC (Areas 9/46) is held to implement higher-order control processes that are superordinate to the more basic vlPFC functions. Specifically, this dlPFC region is held to support the monitoring and manipulation of representations in working memory, which entails the planning and monitoring of intended and expected acts and events, including those related to the first-order executive activities of the vlPFC (Petrides, 2005; Petrides & Pandya, 2002a). In the context of the current results, it is easy to align the vlPFC's involvement in successful conflict adaptation with its proposed function in the process specificity model, as the strategic regulation of the information flow in posterior regions, particularly the ventral visual stream, is precisely the assumed role of frontal top–down influences in the control over conflict in Stroop-type tasks (Botvinick et al., 2001; Cohen, Dunbar, & McClelland, 1990). Moreover, it can also be argued that this model provides a parsimonious account for the additional involvement of the dlPFC and the nature of the relation between activity in this area and behavioral adaptation. From this perspective, the higher-order monitoring and manipulation functions of the dlPFC would quite naturally be recruited when the more basic task-set maintenance operations of the vlPFC run into trouble. The dlPFC might then reinforce the current goal representations that guide the first-order executive processes of the vlPFC. This type of "emergency involvement" of the dlPFC would be expected to be expressed to a greater extent in subjects who are relatively poor at resolving conflict, thus producing the negative association with behavioral adaptation scores observed in the empirical data. Note that this account is necessarily a posteriori and speculative in nature, but it can serve as a useful a priori hypothesis for future neuroimaging and perhaps TMS studies of conflict control.

Finally, it should be pointed out that the right IFG has attracted much attention in recent years as a putative source of inhibitory control processes (reviewed in Aron, 2007; Aron, Robbins, & Poldrack, 2004). Briefly, although this view had originally cast the right IFG as being primarily and directly involved in the suppression of undesirable motor output, recent evidence (Hampshire, Chamberlain, Monti, Duncan, & Owen, 2010; Sharp et al., 2010; Mars, Piekema, Coles, Hulstijn, & Toni, 2007) has necessitated a refinement of this hypothesis, whereby this region is now considered to be involved in updating action plans, of which response inhibition is a common component or variety (Verbruggen, Aron, Stevens, & Chambers, 2010). Although the musings on action inhibition/updating roles of the right IFG have mostly focused on the opercular and triangular aspects of this gyrus (BA 44 and 45; Aron, 2007), the activations attributed to inhibitory processes in many of the neuroimaging studies supporting this view have also tended to bleed into the more anterior and inferior pars orbitalis (BA 47) of the IFG (Chikazoe et al., 2009; Aron & Poldrack, 2006; Garavan, Ross, & Stein, 1999), such that a consideration of the current results in the light of this model seems appropriate.

Could the current findings be reflective of an inhibitory or motor plan updating function of right IFG? We consider this unlikely, mainly because there is no obvious sign of or benefit to response inhibition (or motor plan updating) in adaptation to stimulus conflict. First, the occurrence of conflict on trial $n - 1$ does not indicate any particular response contingencies for trial n, such that no *selective* preparatory inhibition of a specific response would be warranted or advantageous. Second, if conflict on trial $n - 1$ were to trigger nonselective response inhibition, such as a generic shift toward a higher response threshold, this should lead to general slowing of responses on trial n, which is not the case in the empirical data (but see King, Korb, von Cramon, & Ullsperger, 2010). Instead, the conflict adaptation effect reflects a mix of conflict-triggered speeding of responses to incongruent stimuli and slowing of responses to congruent stimuli that can be explained by assuming a reduction in the interfering/facilitating influence of the task-irrelevant stimulus features following conflict-triggered enhancement of top–down

control (Egner, 2007; Botvinick et al., 2001). However, to test the possibility that conflict-driven IFG activity in the current experiments may perhaps be related exclusively to the "slowing component" of the conflict adaptation effect, we correlated individual IFG beta estimates with the degree of postconflict slowing on congruent trials (IC–CC trial RT) and postconflict speeding on incongruent trials (CI–II trial RT), across individuals. In both data sets, conflict-triggered IFG activity was more closely correlated with the speed-up of responses on incongruent trials (Experiment 1: $r = .51$, $p < .05$; Experiment 2: $r = .53$, $p < .05$) than with the slow down of responses on congruent trials (Experiment 1: $r = .34$, $p > .1$; Experiment 2: $r = .15$, $p > .1$). Thus, an interpretation of the current results from an inhibitory or motor plan perspective of right IFG function appears unfeasible.

In conclusion, by employing an individual difference approach in the investigation of the neural bases of conflict-driven control, we have revealed a previously unsuspected key role of the right vlPFC in mediating behavioral adaptation to stimulus conflict, thus enriching our understanding of the mapping of specific executive processes onto the PFC. The respective relations of conflict-driven vlPFC and dlPFC activity with behavioral conflict adaptation across subjects led us to speculate that, in general accordance with Petrides' process specificity model (Petrides, 1994), the vlPFC may be engaged in the primary regulation of stimulus processing (and thus, conflict control), whereas the dlPFC monitoring and manipulation of current working memory content is evoked under conditions where vlPFC-mediated performance is poor.

Acknowledgments

This work was supported by NIMH grant 5R01MH087610-02 (T. E.). I thank my coauthors on the original publications: Amit Etkin, Seth Gale, and Joy Hirsch.

Reprint requests should be sent to Tobias Egner, Duke University, LSRC Box 90999, Durham, NC 27708, or via e-mail: tobias.egner@duke.edu.

REFERENCES

Aron, A. R. (2007). The neural basis of inhibition in cognitive control. *Neuroscientist, 13,* 214–228.

Aron, A. R., & Poldrack, R. A. (2006). Cortical and subcortical contributions to stop signal response inhibition: Role of the subthalamic nucleus. *Journal of Neuroscience, 26,* 2424–2433.

Aron, A. R., Robbins, T. W., & Poldrack, R. A. (2004). Inhibition and the right inferior frontal cortex. *Trends in Cognitive Sciences, 8,* 170–177.

Barbas, H. (1988). Anatomic organization of basoventral and mediodorsal visual recipient prefrontal regions in the rhesus monkey. *Journal of Comparative Neurology, 276,* 313–342.

Botvinick, M. M., Braver, T. S., Barch, D. M., Carter, C. S., & Cohen, J. D. (2001). Conflict monitoring and cognitive control. *Psychological Review, 108,* 624–652.

Carmichael, S. T., & Price, J. L. (1995). Sensory and premotor connections of the orbital and medial prefrontal cortex of macaque monkeys. *Journal of Comparative Neurology, 363,* 642–664.

Chikazoe, J., Jimura, K., Asari, T., Yamashita, K., Morimoto, H., Hirose, S., et al. (2009). Functional dissociation in right inferior frontal cortex during performance of go/no-go task. *Cerebral Cortex, 19,* 146–152.

Cohen, J. D., Dunbar, K., & McClelland, J. L. (1990). On the control of automatic processes: A parallel distributed processing account of the Stroop effect. *Psychological Review, 97,* 332–361.

Cohen, L., Dehaene, S., Naccache, L., Lehericy, S., Dehaene-Lambertz, G., Henaff, M. A., et al. (2000). The visual word form area: Spatial and temporal characterization of an initial stage of reading in normal subjects and posterior split-brain patients. *Brain, 123,* 291–307.

di Pellegrino, G., Ciaramelli, E., & Ladavas, E. (2007). The regulation of cognitive control following rostral anterior cingulate cortex lesion in humans. *Journal of Cognitive Neuroscience, 19,* 275–286.

Egner, T. (2007). Congruency sequence effects and cognitive control. *Cognitive, Affective & Behavioral Neuroscience, 7,* 380–390.

Egner, T. (2008). Multiple conflict-driven control mechanisms in the human brain. *Trends in Cognitive Sciences, 12,* 374–380.

Egner, T., Etkin, A., Gale, S., & Hirsch, J. (2008). Dissociable neural systems resolve conflict from emotional versus nonemotional distracters. *Cerebral Cortex, 18,* 1475–1484.

Egner, T., & Hirsch, J. (2005a). Cognitive control mechanisms resolve conflict through cortical amplification of task-relevant information. *Nature Neuroscience, 8,* 1784–1790.

Egner, T., & Hirsch, J. (2005b). The neural correlates and functional integration of cognitive control in a Stroop task. *Neuroimage, 24,* 539–547.

Ekman, P., & Friesen, W. V. (1976). *Pictures of facial affect*. Palo Alto, CA: Consulting Psychologists.

Etkin, A., Egner, T., Peraza, D. M., Kandel, E. R., & Hirsch, J. (2006). Resolving emotional conflict: A role for the rostral anterior cingulate cortex in modulating activity in the amygdala. *Neuron, 51,* 871–882.

Fellows, L. K., & Farah, M. J. (2005). Is anterior cingulate cortex necessary for cognitive control? *Brain, 128,* 788–796.

Forstmann, B. U., Jahfari, S., Scholte, H. S., Wolfensteller, U., van den Wildenberg, W. P., & Ridderinkhof, K. R. (2008). Function and structure of the right inferior frontal cortex predict individual differences in response inhibition: A model-based approach. *Journal of Neuroscience, 28,* 9790–9796.

Forstmann, B. U., van den Wildenberg, W. P., & Ridderinkhof, K. R. (2008). Neural mechanisms, temporal dynamics, and individual differences in interference control. *Journal of Cognitive Neuroscience, 20,* 1854–1865.

Fuster, J. M. (2008). *The prefrontal cortex* (4th ed.). London: Academic Press.

Garavan, H., Ross, T. J., & Stein, E. A. (1999). Right hemispheric dominance of inhibitory control: An event-related functional MRI study. *Proceedings of the National Academy of Sciences, U.S.A., 96,* 8301–8306.

Goldman-Rakic, P. S. (1987). Circuitry of the prefrontal cortex and the regulation of behavior by representational memory. In F. Plum & V. B. Mountcastle (Eds.), *Handbook of physiology: Section 1. The nervous system*

(Vol. 5, pp. 373–417). Bethesda, MD: American Physiological Society.
Goldman-Rakic, P. S. (1996). The prefrontal landscape: Implications of functional architecture for understanding human mentation and the central executive. *Philosophical Transactions of the Royal Society of London, Series B, Biological Sciences, 351,* 1445–1453.
Goldman-Rakic, P. S., & Leung, H. C. (2002). Funtional architecture of the dorsolateral prefrontal cortex. In D. T. Stuss & R. T. Knight (Eds.), *Principles of frontal lobe function* (1st ed., pp. 85–95). New York: Oxford University Press.
Gratton, G., Coles, M. G., & Donchin, E. (1992). Optimizing the use of information: Strategic control of activation of responses. *Journal of Experimental Psychology: General, 121,* 480–506.
Hampshire, A., Chamberlain, S. R., Monti, M. M., Duncan, J., & Owen, A. M. (2010). The role of the right inferior frontal gyrus: Inhibition and attentional control. *Neuroimage, 50,* 1313–1319.
Hommel, B., Proctor, R. W., & Vu, K. P. (2004). A feature-integration account of sequential effects in the Simon task. *Psychological Research, 68,* 1–17.
Kanwisher, N., McDermott, J., & Chun, M. M. (1997). The fusiform face area: A module in human extrastriate cortex specialized for face perception. *Journal of Neuroscience, 17,* 4302–4311.
Kerns, J. G., Cohen, J. D., MacDonald, A. W., III, Cho, R. Y., Stenger, V. A., & Carter, C. S. (2004). Anterior cingulate conflict monitoring and adjustments in control. *Science, 303,* 1023–1026.
Kerns, J. G., Cohen, J. D., MacDonald, A. W., III, Johnson, M. K., Stenger, V. A., Aizenstein, H., et al. (2005). Decreased conflict- and error-related activity in the anterior cingulate cortex in subjects with schizophrenia. *American Journal of Psychiatry, 162,* 1833–1839.
King, J. A., Korb, F. M., von Cramon, D. Y., & Ullsperger, M. (2010). Posterror behavioral adjustments are facilitated by activation and suppression of task-relevant and task-irrelevant information processing. *Journal of Neuroscience, 30,* 12759–12769.
Kriegeskorte, N., Simmons, W. K., Bellgowan, P. S., & Baker, C. I. (2009). Circular analysis in systems neuroscience: The dangers of double dipping. *Nature Neuroscience, 12,* 535–540.
Mars, R. B., Piekema, C., Coles, M. G., Hulstijn, W., & Toni, I. (2007). On the programming and reprogramming of actions. *Cerebral Cortex, 17,* 2972–2979.
Mayr, U., Awh, E., & Laurey, P. (2003). Conflict adaptation effects in the absence of executive control. *Nature Neuroscience, 6,* 450–452.
Miller, E. K., & Cohen, J. D. (2001). An integrative theory of prefrontal cortex function. *Annual Review of Neuroscience, 24,* 167–202.
Norman, D. A., & Shallice, T. (1986). Attention to action: Willed and automatic control of behavior. In G. E. Schwarz & D. Shapiro (Eds.), *Consciousness and self-regulation* (Vol. 4, pp. 1–18). New York: Plenum Press.
Petrides, M. (1994). Frontal lobes and working memory: Evidence from investigations of the effects of cortical excisions in nonhuman primates. In F. Boller & J. Grafman (Eds.), *Handbook of neuropsychology* (pp. 59–84). Amsterdam: Elsevier.
Petrides, M. (1996). Specialized systems for the processing of mnemonic information within the primate frontal cortex. *Philosophical Transactions of the Royal Society of London, Series B, Biological Sciences, 351,* 1455–1461; discussion 1461-1462.
Petrides, M. (2005). Lateral prefrontal cortex: Architectonic and functional organization. *Philosophical Transactions of the Royal Society of London, Series B, Biological Sciences, 360,* 781–795.
Petrides, M., & Pandya, D. N. (1994). Comparative architectonic analysis of the human and the macaque frontal cortex. In F. Boller & J. Grafman (Eds.), *Handbook of neuropsychology* (Vol. 9, pp. 17–58). Amsterdam: Elsevier.
Petrides, M., & Pandya, D. N. (2002a). Association pathways of the prefrontal cortex and functional observations. In D. T. Stuss & R. T. Knight (Eds.), *Principles of frontal lobe function* (1st ed., pp. 31–50). New York: Oxford University Press.
Petrides, M., & Pandya, D. N. (2002b). Comparative cytoarchitectonic analysis of the human and the macaque ventrolateral prefrontal cortex and corticocortical connection patterns in the monkey. *European Journal of Neuroscience, 16,* 291–310.
Shallice, T., & Burgess, P. (1996). The domain of supervisory processes and temporal organization of behaviour. *Philosophical Transactions of the Royal Society of London, Series B, Biological Sciences, 351,* 1405–1411; discussion 1411-1402.
Sharp, D. J., Bonnelle, V., De Boissezon, X., Beckmann, C. F., James, S. G., Patel, M. C., et al. (2010). Distinct frontal systems for response inhibition, attentional capture, and error processing. *Proceedings of the National Academy of Sciences, U.S.A., 107,* 6106–6111.
Stuss, D. T., & Benson, D. F. (1984). Neuropsychological studies of the frontal lobes. *Psychological Bulletin, 95,* 3–28.
Stuss, D. T., Floden, D., Alexander, M. P., Levine, B., & Katz, D. (2001). Stroop performance in focal lesion patients: Dissociation of processes and frontal lobe lesion location. *Neuropsychologia, 39,* 771–786.
Verbruggen, F., Aron, A. R., Stevens, M. A., & Chambers, C. D. (2010). Theta burst stimulation dissociates attention and action updating in human inferior frontal cortex. *Proceedings of the National Academy of Sciences, U.S.A., 107,* 13966–13971.